ARTICLE

Conformational equilibria in *o*-anisic acid ant its monohydrated complex, the prevalence of the *trans*-COOH form

Received 00th January 20xx,
Accepted 00th January 20xx

DOI: 10.1039/x0xx00000x

Juan Carlos López,*[a] Alberto Macario [a] Susana Blanco *[a]

The conformation of *ortho*-anisic acid and its monohydrated clusters have been studied by rotational spectroscopy in a supersonic jet to analyze the structural implications of *ortho* substitution. The dominant species shows a *trans*-COOH arrangement stabilized by an intramolecular hydrogen bond O-H···O from the acid to the methoxy group. The spectra of two non-planar skeleton monomer forms with a *cis*-COOH arrangement have been observed including a tunneling doublet for the most stable one. The periodic potential energy function for the COOH internal rotation connecting these *cis* forms has been estimated from the experimental data. For the first time a water complex with an acid in *trans*-COOH form has been observed. This is more abundant than another weak *cis*-COOH water complex form observed. The observation of the rotational spectra of salicylic acid, methyl salicylate and methyl 2-methoxybenzoate, formed upon heating of *o*-anisic acid gives an additional interest to the chemistry of *ortho* substituted benzoic acids.

Introduction

Hydrogen bond (HB) is one of the main interacting forces existing in nature,[1] being especially important in the biological media. It is responsible for molecular recognition and plays and important role in the structural behavior of biological macromolecules.[2] The role of water as the leading solvent and the main biological matrix[1] should be related to its small size and proton donor/acceptor character, which confers to it an enormous potential to form HBs. Polar functional groups as carboxylic acid (–COOH), which may adopt *cis* or *trans* configuration, have also a double donor/acceptor HB character. The *cis*-COOH form is the most stable arrangement[3] and it is responsible of the preference of acids to form dimers[4] or sequential cycles with water molecules through O-H···O HBs.[5,6] The *trans*-COOH form is rarely observed[7] except when it is stabilized by an HB to a neighbor polar group as occur for the type II conformers of aminoacids,[8,9] where an intramolecular O-H···N HB is present. However, in the presence of water only the *cis*-COOH forms are usually stabilized even in supersonic expansions, as it was observed for microsolvated glycine[10] and alanine.[11]

Ortho-subtituted benzoic acids include several examples of carboxylic groups with a polar neighbor groups. One of these is *ortho*-anisic acid (2-methoxybenzoic acid, ANI) a natural compound that acts as inhibitor of bacterial growth[12] and influences the catalytic activity of enzymes.[13] ANI has the acid and methoxy groups close enough to allow for the establishment of a HB intramolecular interaction between them (see Figure 1). Previous experimental studies[14] report the existence in solution of only the *trans* form. X-ray analyses[15] revealed that in the solid state only the dimer formed from monomers in the *cis* configuration is present. This system has been included in computational studies to analyze the formation of intramolecular hydrogen bonds[16] or related to the *ortho* effect,[17] a not very clear concept that tries to explain the differences in reactivity of benzene *ortho*-derivatives with respect to those of their *meta*- and *para*-isomers. The *ortho* effect is attributed to arise from contributions of inductive and resonance effects transmitted through the ring in addition to steric effects. The non-applicability of Hammet equation[17] to *ortho* compounds or the different fragment patterns observed in mass spectrometry[18] of *ortho* compounds are known examples.

In the present work, we have analyzed the *cis-trans* equilibrium of ANI and its monohydrated complexes using Fourier transform microwave spectroscopy (FTMW) coupled to supersonic expansion. This technique has proved to be an excellent tool to determine the molecular structure of gas-phase molecules or their complexes and to identify the non-covalent interactions involved in cluster formation.[19] Chirped-pulse FTMW spectroscopy is especially useful to identify the different species present in the jet since it provides a direct snapshot of all the polar species present in the supersonic expansion.[20,21] The structural details provided by this technique would give new insight into the different forces conferring distinctive properties to *ortho* compounds. The fact that the only observed form in solution is the *trans*-COOH form is a challenge to observe a water complex with an acid showing such an arrangement.

[a] Departamento de Química Física y Química Inorgánica, Facultad de Ciencias, Universidad de Valladolid, 47011 Valladolid, Spain. E-mail: jclopez@qf.uva.es , sblanco@qf.uva.es

Electronic Supplementary Information (ESI) available: [details of any supplementary information available should be included here]. See DOI: 10.1039/x0xx00000x

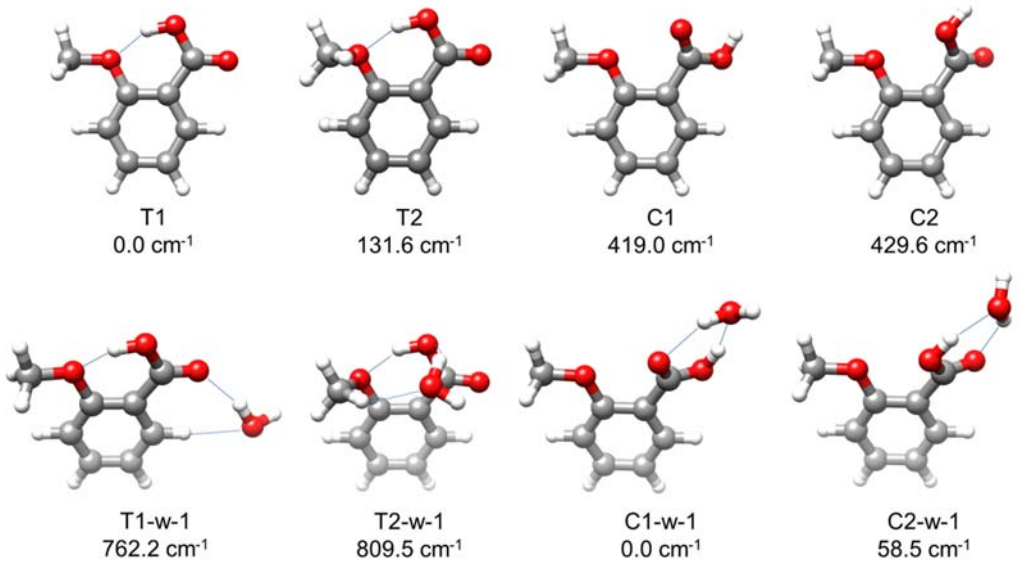

Fig. 1 The most stable trans (T) and cis (C) conformations of ANI and their monohydrated complexes predicted at MP2/6-311++G(d,p) level. The relative energies are referred to the most stable forms.

Experimental and computational methods

Microwave spectroscopy

A commercial sample of ANI (b.p. 99-100ºC) was vaporized using a heating nozzle (~110ºC). Water (or commercial samples of D_2O or $H_2{}^{18}O$) was placed in a reservoir inserted in the gas line. The carrier gas was Ar or Ne at backing pressures ranging to 4 bar expanding through a 0.8 mm nozzle in pulses of 700-900 μs duration. The ANI isotopic species were measured in their natural abundance, except the deuterated species and the ^{18}O of the water which were generated using D_2O and $H_2{}^{18}O$. The rotational spectra were recorded using a broadband CP-FTMW spectrometer[22] in the 2 to 8 GHz and a molecular beam FTMW spectrometer[23] in the 4 to 16 GHz. In the CP-FTMW spectrometer the spectra were recorded in steps of 2 GHz. Chirp pulses of 4 μs were created by an arbitrary waveform generator and amplified to 20 W. The polarization signal was radiated from a horn antenna in a direction perpendicular to that of the expanding gas. A molecular transient emission spanning 40 μs is then detected through a second horn, recorded with a digital oscilloscope and Fourier-transformed to the frequency domain. The accuracy of frequency measurements is better than 10 kHz. In the MB-FTMW instrument, short (typ. 0.3 μs, 10-300 mW) microwave pulses were used for polarization purposes. Typically, a *ca.* 400 μs-length time domain spectrum was recorded in 40-100 ns intervals and converted to the frequency domain by a fast Fourier transform. Due to the collinear arrangement of the jet and resonator axis each rotational transition splits in two Doppler components so the resonant frequencies are taken as the arithmetic mean of both components. Frequency accuracy is better than 5 kHz. The rotational spectra of the $H_2{}^{18}O$ isotopologues were recorded in the MB-FTMW spectrometer. The spectra of the deuterated species were recorded in the CP-FTMW instrument.

Complementary ESI-TOF and GC/MS measurements were done for the sample before and after heating to test the presence of recombination products.

Computational methods

Prior to analyze the rotational spectra, theoretical investigations[24] of the potential energy surface (PES) of ANI and its monohydrated cluster, which show rich conformational landscapes, were done initially at MP2/6-311++G(d,p) level. In a second step the most stable forms were further investigated at B3LYP/6-311++G(d,p), MP2/aug-cc-pVDZ or CCSD/6-311G(d,p) levels to test their performance. The four most stable conformers of the monomer and their corresponding most stable monohydrated complexes are shown in Figure 1. Complete data sets are collected in the ESI (Tables S1-S4, Figures S1-S2).

Results and discussion

Rotational Spectrum

The rotational spectrum shows a high density of lines. As illustrated in Figure 2, the search for the monomer spectra lead to the assignment of four different species, three of which were identified as the ground state of conformers T1, C2 and C1. The weakest lines correspond to an excited vibrational state associated to form C2 (C2-exc).

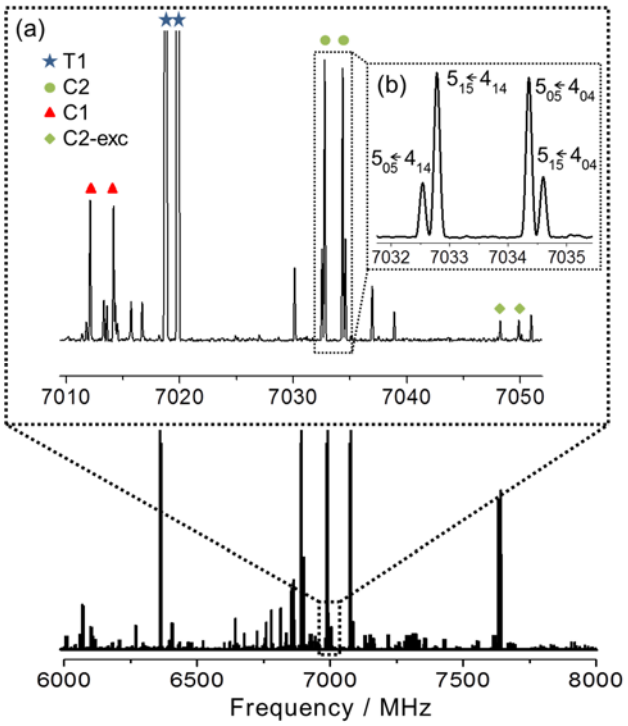

Fig. 2 CP-FTMW, 6-8 GHz, rotational spectra of ANI. The (a) zoom region shows the frequency and intensity patterns for the different monomer species. The (b) zoom shows a typical μ_a- and μ_b-type quadruplet.

The identification of T1 was confirmed by the measurements of all monosubstituted ^{13}C and methoxy-^{18}O isotopologues spectra in their natural abundance and the –COOD species. The identification of C2 was confirmed by the identification of the –COOD species. Relative intensity measurements[25] allow us to estimate the relative population ratios for the monomer conformers $N_{T1}/N_{C2}/N_{C1}/N_{C2exc}$~100/59(5)/18(3)/8(2). To do this the values of the calculated electric dipole moment components were used.

Subsequent search on the spectrum lead to the assignments of the monohydrated species T1-w-1 and the identification of the spectra of species structurally similar to ANI: methyl 2-methoxybenzoate,[26] salicylic acid,[27] methyl salicylate[28] and some of their water complexes.[29] Finally very weak signals were assigned to C2-w-1 ANI-water complex. For T1-w-1 the spectra of diverse isotopologues of water, $H_2{}^{18}O$, DHO and D_2O and COOD were also measured. The relative population ratio of the ANI-water forms was estimated to be $N_{T1\text{-}w\text{-}1}/N_{C2\text{-}w\text{-}1}$=100/24(5). All the spectra were analyzed using Watson[30] A-reduced semirigid rotor Hamiltonian in the I^r representation. The resulting spectroscopic parameters for the parent species are given in Table 1. (The complete datasets are given in tables S5-S31).

Table 1 Rotational parameters obtained from the analysis of the spectrum of all the observed species of ANI monomer and their water complexes.

Fitted Parameters[a]	T1	C2	C1	C2-exc	T1-w-1	C2-w-1
A/MHz	1387.631149(48)[b]	1397.17908(17)	1404.22981(39)	1396.55339(66)	1255.08080(16)	1384.48829(73)
B/MHz	1172.426068(43)	1155.97828(11)	1145.60774(30)	1154.40677(30)	656.263660(55)	610.48530(30)
C/MHz	638.664972(40)	640.89394(10)	638.99426(13)	642.75248(17)	432.826830(49)	428.58680(12)
P_{cc}/uÅ^2	1.975701(39)	5.17393(10)	5.07249(19)	6.69260(25)	2.56390(12)	6.84282(46)
Δ_J/kHz	0.05698(43)	0.0670(16)	0.0467(25)	0.0211(19)	0.0868(29)	0.0475(27)
Δ_{JK}/kHz	-0.08210(37)	-0.0396(18)	-	-	-0.1493(91)	-
Δ_K/kHz	0.03139(52)	-	-	-	0.0787(61)	-0.0352(27)
δ_J/kHz	-0.001822(52)	0.00141(37)	0.0111(14)	-	0.0071(16)	-
δ_K/kHz	-0.02248(57)	-0.2185(27)	0.0875(72)	-0.103(19)	0.0236(43)	-0.0204(46)
N	256	105	48	25	149	46
σ/kHz	4.5	4.7	4.6	4.1	4.0	5.5

[a] A, B and C are the rotational constants. P_{cc} is the planar moment of inertia in the *ab* plane, derived from $P_{cc}=(I_a+I_b-I_c)/2$. Δ_J, Δ_{JK}, Δ_K, δ_J and δ_K are the quartic centrifugal distortion constants. N is the number of rotational transitions fitted. σ is the rms deviations of the fit. [b] Standard error is given in parentheses in units of the last digits.

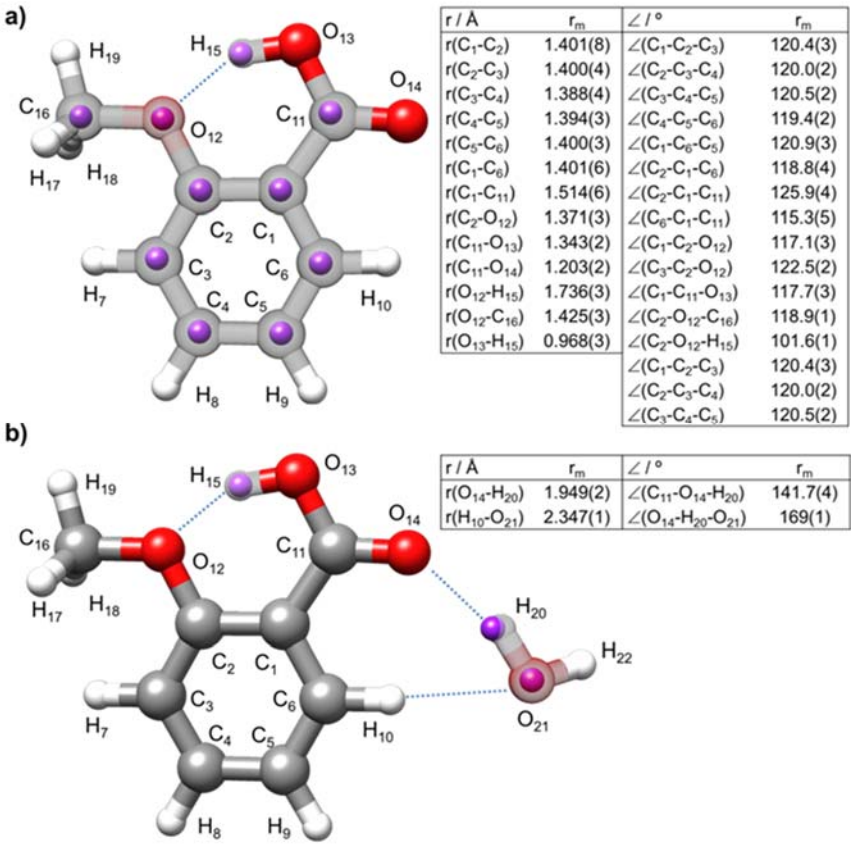

r / Å	r_m	∠ / °	r_m
$r(C_1-C_2)$	1.401(8)	$\angle(C_1-C_2-C_3)$	120.4(3)
$r(C_2-C_3)$	1.400(4)	$\angle(C_2-C_3-C_4)$	120.0(2)
$r(C_3-C_4)$	1.388(4)	$\angle(C_3-C_4-C_5)$	120.5(2)
$r(C_4-C_5)$	1.394(3)	$\angle(C_4-C_5-C_6)$	119.4(2)
$r(C_5-C_6)$	1.400(3)	$\angle(C_1-C_6-C_5)$	120.9(3)
$r(C_1-C_6)$	1.401(6)	$\angle(C_2-C_1-C_6)$	118.8(4)
$r(C_1-C_{11})$	1.514(6)	$\angle(C_2-C_1-C_{11})$	125.9(4)
$r(C_2-O_{12})$	1.371(3)	$\angle(C_6-C_1-C_{11})$	115.3(5)
$r(C_{11}-O_{13})$	1.343(2)	$\angle(C_1-C_2-O_{12})$	117.1(3)
$r(C_{11}-O_{14})$	1.203(2)	$\angle(C_3-C_2-O_{12})$	122.5(2)
$r(O_{12}-H_{15})$	1.736(3)	$\angle(C_1-C_{11}-O_{13})$	117.7(3)
$r(O_{12}-C_{16})$	1.425(3)	$\angle(C_2-O_{12}-C_{16})$	118.9(1)
$r(O_{13}-H_{15})$	0.968(3)	$\angle(C_2-O_{12}-H_{15})$	101.6(1)
		$\angle(C_1-C_2-C_3)$	120.4(3)
		$\angle(C_2-C_3-C_4)$	120.0(2)
		$\angle(C_3-C_4-C_5)$	120.5(2)

r / Å	r_m	∠ / °	r_m
$r(O_{14}-H_{20})$	1.949(2)	$\angle(C_{11}-O_{14}-H_{20})$	141.7(4)
$r(H_{10}-O_{21})$	2.347(1)	$\angle(O_{14}-H_{20}-O_{21})$	169(1)

Fig. 3 The experimental r_s structure (purple) of the T1 conformer compared to the CCSD/6-311++G(d,p) r_e structure. A selection of the r_m bond lengths (r) and angles (∠) are given. **b)** For the T1-w-1 complex the r_s data are compared to the MP2/6-311++G(d,p) r_e structure.

Molecular Structure

The values of the planar moment P_{cc} (see Tables 1, S5-S8) for the parent and isotopologues allow concluding that conformer T1 and its water complex T1-w-1 have planar skeletons. For T1 species the P_{cc} value, not far from that of anisole,[31] comes from the contribution of the methyl group out-of-plane hydrogen atoms. The substitution, r_s,[32,33] and mass dependence, r_m,[34] structures have been determined from the spectra of the different isotopologues for T1 and T1-w-1 species as summarized in Figure 3. The complete results and the details of these calculations are given in the ESI tables S32-S36, where they are compared to the r_e structures calculated at different levels of theory. The distortions of the ring associated to alteration of the ring resonance and to the inductive effects due to the *ortho* substituents are apparent from these structures. However, alternation is appreciable only for the ring-angles.[31] The short OH···O bond distance of 1.736(3) Å indicates a strong hydrogen bond probably stabilized by resonance.[1,35]

The planar moment P_{cc} values for the *cis*-COOH species suggest a non-planar skeleton. Theoretical calculations predict a torsion of the –COOH group around the C-C bond which forces the carboxylic oxygen atoms to be out of the ring plane. The r_s coordinates of the carboxylic hydrogen atom of C2 form corroborates the identification of this form (see Table S33) which is more stable than C1 according to the observed intensities. The theoretical calculations at the different levels show discrepancies between them and with the experimental results as deduced from the observed and predicted values of P_{cc} or the stabilization energies. Using the DFT structure, the experimental value of P_{cc} is approximately reproduced for dihedral angles $\angle C_2C_1C_{11}O_{13}$ or $\angle C_2C_1C_{11}O_{14}$ of *ca.* ±18º. In the same way the estimated dihedral angle $\angle C_2C_1C_{11}O_{13}$ for C2-w-1 is of 21º.

Potential Energy Function of *cis* forms

A deeper insight on the C1/C2 conformational equilibria comes from the PES associated to the torsion of the COOH group around the C_1-C_{11} bond which interconverts both forms. Theoretical calculations give different PESs (see Figure 4) which can be well described by a periodical function on the angle $\tau = \angle C_2C_1C_{11}O_{13}$ - 90°:

$$V(\tau) = V(0) + \frac{V(1)}{2}(1 - sin\tau) + \frac{V(2)}{2}(1 - cos2\tau) + \frac{V(4)}{2}(1 - cos4\tau) \quad (1)$$

This function has equivalent maxima at values of τ = 0º and 180º with the COOH plane perpendicular to the aromatic ring. It exhibits two locally symmetric double minimum wells with small barriers at the planar skeleton forms with τ = 90º

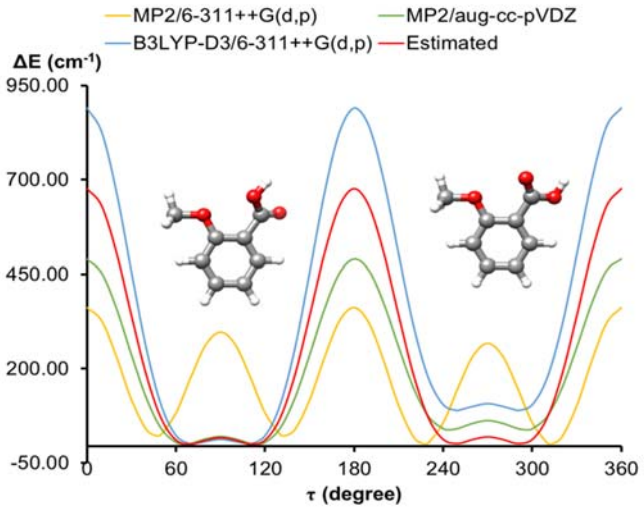

Fig. 4 Predicted and estimated Periodic potential energy functions for the rotation of the COOH group around the C_1-C_{11} bond ($\tau = \angle C_2C_1C_{11}O_{13}$ - 90º) that interconverts C1 and C2 forms.

and 270º. These local double minimum wells have different energies between them and can be associated to conformers C1 and C2. We have explored this PES using the flexible model of Meyer[36,37] with the B3LYP-D3/6-311++G(d,p) structural relaxation parameters (see Table S37). The experimental rotational constants and P_{cc} values are well reproduced for the function:

$$V(\tau) = 637 + \frac{0.5}{2}(1 - sin\tau) - \frac{620}{2}(1 - cos2\tau) - \frac{216}{2}(1 - cos4\tau)\ cm^{-1} \quad (2)$$

which is compared to the theoretical ones in Figure 4. The result are given in Table 2 where they are compared to those from theoretical functions. For the experimentally estimated function the energy ordering E(C2)<E(C1)<E(C2-exc) is in agreement with the observed intensities in the rotational spectrum (see Figure 2). This energy order holds up to V(1)=3.5 cm^{-1}. The estimated barrier at τ = 0º and 180º is of 637 cm^{-1} and those at τ = 90º and 270º of 17 cm^{-1}. The minima occur at dihedral angles $\angle C_2C_1C_{11}O_{13}$ of ±22º for C2 or 180º ± 22º for C1. The double minimum well shapes are intermediate between those calculated at B3LYP-D3/6-311++G(d,p) and MP2/aug-cc-PVDZ levels**.** The experimental estimation yields a small difference between forms C1 and C2, being C2 the most stable.

The COOH group torsion PES is the result of a delicate balance between the resonance stabilization and the steric hindrance the methoxy and carboxylic groups. The differences between the theoretical and experimental results shown here indicate that this balance is very critical. A comparison of the MP2/aug-cc-pVDZ torsional functions in benzoic acid and ANI allows an estimation of the hindrance forces as shown in Figure 5.

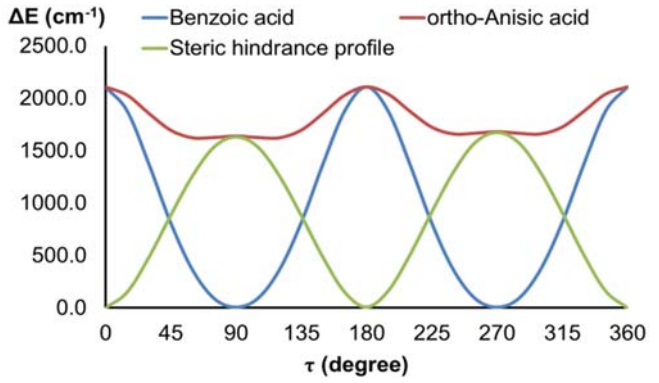

Fig. 5 Estimation of the steric hindrance forces or ortho effect (green) taken by the comparison of the torsional function of benzoic acid (blue) and the C2/C1 interconversion function of ANI (red), both of them predicted at MP2/aug-cc-pVDZ level of theory.

Table 2 (a) Parameters describing the potential energy function for the cis–COOH internal rotation of o-anisic acid (see eq. (1)) predicted at B3LYP/6-311++G(d,p) (DFT), MP2/aug-cc-pVDZ (MP2) or estimated from flexible model (eq. 2). (b) Flexible model predictions for the observed vibrational states C2, C2-exc and C1.

	DFT	MP2	Eq. (2)	
a) Potential functions				
V(0)/cm^{-1}	842.7	468.9	637.4	
V(1)/cm^{-1}	95.0	42.0	0.5	
V(2)/cm^{-1}	-830.2	-448.5	-620.4	
V(4)/cm^{-1}	-272.1	-174.5	-215.6	
b) Flexible model predictions for the vibrational states				
C2				Exp.
E_0/cm^{-1}	9.18	10.92	10.35	
A_0/MHz	1398.54	1397.02	1397.81	1397.179
B_0/MHz	1156.63	1153.38	1155.10	1155.978
C_0/MHz	639.62	642.03	640.75	640.894
$P_{cc\,0}$/uÅ^2	4.09	6.38	5.17	5.1739
C2-exc				Exp.
E_1/cm^{-1}	14.94	12.98	13.77	
A_1/MHz	1397.43	1396.21	1396.81	1396.554
B_1/MHz	1154.31	1151.52	1152.93	1154.407
C_1/MHz	641.34	643.38	642.35	642.752
$P_{cc\,1}$/uÅ^2	5.73	7.67	6.69	6.6926
C1				Exp.
E_0/cm^{-1}	100.52	50.01	10.92	
A_0/MHz	1404.84	1402.30	1404.53	1404.230
B_0/MHz	1144.72	1141.73	1144.37	1145.608
C_0/MHz	638.44	640.62	638.69	638.994
$P_{cc\,0}$/uÅ^2	4.82	7.07	5.09	5.072

Conclusions

The present microwave study of ANI shows a number of interesting features about its structure and dynamics. The dominant form in the spectrum is T1 where a HB from the acid group to the methoxy oxygen overcomes the conformational energy increase to adopt a *trans*-COOH arrangement. However, the C1 and C2 forms with a *cis* arrangement of the COOH group have been also observed showing appreciable intensities giving a total abundance ratio *trans* : *cis* = 1 : 0.78. This is in contrast with the observation of only the T1 form in solution[14] or only the C1 form in the dimers observed in the solid state.[15] In the gas-phase C2 results to be slightly more stable than C1. The T2 form (see Figure 1), predicted to be more stable than the *cis*-COOH forms has not been observed. This can be attributed to collisional relaxation to the T1 form in the jet due to a small barrier to the rotation of the methoxy group around C_2-O_{12} bond as shown in Figure S3.[38]

Ortho effect[17] has been described to arise from contributions of inductive and resonance effects transmitted through the ring and steric interaction between the adjacent groups. In conformer T1 the OH···O HB dominates and forces a planar skeleton. For the C1/C2 forms, the features of the PES for COOH torsion described above give a measure of the steric repulsions between the oxygen atom of methoxy and those of the acid group (Figure 5). In addition, the observation of salicylic acid, methyl salicylate and methyl 2-methoxybenzoate upon heating of ANI, would enter into the range of definitions of the *ortho* effect of mass spectrometry.[18] These explain the different fragment patterns observed in mass spectrometry of *ortho* compounds though a mechanistic view. The possible donor-acceptor interactions between substituents would give rise to transition states that allow the transfer of atoms or molecular fragments between the interacting groups. In fact, the conversion of ANI into salicylic acid, methyl salicylate or methyl-2-methoxybenzoate involves exchange of a hydrogen atom and a -CH_3 group. Isodesmic reactions to obtain methyl salicylate or salicylic acid plus methyl-2-methoxybenzoate from ANI are predicted to be exothermic and spontaneous.

We have observed two forms of the complex: T1-w-1 and C2-w-1 respectively (see Figure 1). For T1-w-1 water forms a HB O-H···O=C to the carbonyl oxygen of the acid group. This is further stabilized by a weak C-H···O interaction with the closest ring benzene hydrogen atoms. In the C2-w-1 complex water interacts with the acid group forming a sequential cycle with the COOH. The non-bonded water HB may adopt two non-equivalent orientations giving rise to forms C2-w-1 and C2-w-2 (see figure S2). We have assumed that the form observed is C2-w-1 in which the non-bonded hydrogen atom points to the ring plane. Giving the weakness of the spectrum of C2-w-1 the possible spectrum of C1-w-1 is below the detection limit.

The estimated abundances indicate that T1-w-1 is four times more abundant that C2-w-1 in the jet. This is in contrast to the predicted energies for these conformers (see Figure 1) which establishes that the *cis*-COOH water complexes in equilibrium would be dominant. It is well known that after complex formation in the supersonic jet the collisional rate decreases rapidly in the first stages of the expansion, precluding relaxation to equilibrium. In those cases, a kinetic mechanism dominates and the complex formed with preference correspond to the most abundant monomers forms originating the complexes. This seems to be the present case, but it should be mentioned here that the T1 forms are those observed also in solution, so that means that breaking the intermolecular O-H···O would require a high activation energy. In related systems as the amino acids the monomers with and without intramolecular O-H···N bonds are observed in the gas-phase. However in the complexes with water only the *cis*-COOH forms are observed. This reveals the importance of the observation of form T1-w-1 complex, which to our knowledge is the first organic *trans*-COOH acid-water complex observed up to now.

Conflicts of interest

Authors declare that there are no conflicts of interest.

Acknowledgements

The authors acknowledge the Ministerio de Economía y Competitividad (Grant CTQ2016-75253-P) for financial support. A. M. acknowledges the University of Valladolid for the Ph. D. grant (Contratos Predoctorales UVa)..

Notes and references

1 G. A. Jeffrey in *An Introduction to Hydrogen Bonding*, Oxford University Press: New York, **1997**.
2 D. Leckband, J. Israelachvili in *Intermolecular Forces in Biology*, Cambridge University Press: United Kingdom, **2001**.
3 A. G. Császár, W. D. Allen, H. F. Schaefer, *J. Chem. Phys.* **1998**, 108, 9751-9764.
4 W. Li, L. Evangelisti, L. Gou, W. Caminati, R. Meyer, *Angew. Chem. Int. Ed.* **2019**, 131, 869-875.
5 B. Ouyang, T. G. Starkey, B. J. Howard, *J. Phys. Chem. A* **2007**, 111, 6165-6575.
6 B. Ouyang, B. J. Howard, *J. Phys. Chem. A* **2010**, 114, 4109-4117.
7 E. M. S. Maçoas, L. Khriachtchev, M. Petterson, R. Fausto, M. Räsänen, *J. Am. Chem. Soc.* **2003**, 125, 16188-16189.
8 J. C. López, J. L. Alonso, *Top. Curr. Chem.* **2014**, 335-401.
9 S. Blanco, M. E. Sanz, J. C. López, J. L. Alonso, *Proc. Natl. Acad. Sci. USA* **2007**, 104, 20183-20188.
10 J. L. Alonso, E. J. Cocinero, A. Lesarri, M. E. Sanz, J. C. López, *Angew. Chem. Int. Ed.* **2006**, 45, 3471-3474.
11 V. Vaquero, M. E. Sanz, I. Peña, S. Mata, C. Cabezas, J. C. López, J. L. Alonso, *J. Phys. Chem. A* **2014**, 118, 2584-2590.
12 S. Kanchan, D. N. S. Jayachandra, *Can. J. Bot.* **1981**, 59, 199-202.
13 J. F. Lynas, B. Walker, *Bioorg. Med. Chem. Lett.* **1997**, 7, 1133-1138.
14 O. Exner, P. Fiedler, M. Budesinský, J. Kulhánek, *J. Org. Chem.* **1999**, 64, 3513-3518.
15 M. Parvez, *Acta Crystallogr. Sect. C* **1987**, 43, 2243-2245.
16 I. I. Schuter, *J. Chem. Soc., Perkin Trans.* **2002**, 2, 1961-1966.
17 S. Böhm, P. Fiedler, O. Exner, *New J. Chem.* **2004**, 28, 67-74.
18 F. Jariwala, M. Figus, A. Attygalle, *J. Am. Chem. Soc. Mass. Spectrom.* **2011**, 19, 1114-1118.

19 S. Blanco, P. Pinacho, J. C. López, *Angew. Chem. Int. Ed.* **2016**, 55, 9331-9335.
20 C. Pérez, M. T. Muckle, D. P. Zaleski, N. A. Seifert, B. Temelso, G. C. Shields, Z. Kisiel, B. H. Pate, *Science* **2012**, 336, 897-901.
21 J. C. López, C. Pérez, S. Blanco, V. A. Shubert, B. Temelso, G. C. Shields, M. Schnell, *Phys. Chem. Chem. Phys.* **2019**, in press, DOI: 10.1039/c8cp05552a
22 G. G. Brown, B. C. Dian, K. O. Douglass, S. M. Geyer, S. T. Shipman, B. H. Pate, *Rev. Sci. Instrum.* **2008**, 79, 053103.
23 J. L. Alonso, F. J. Lorenzo, J. C. López, A. Lesarri, S. Mata, H. Dreizler, *Chem. Phys.* **1997**, 218, 267-275.
24 Gaussian 09 (Revision B.01), M. J. Frisch, G. W. Trucks, H. B. Schlegel, G. E. Scuseria, M. A, Robb, J. R. Cheeseman, G. Scalmani, V. Barone, B. Mennucci, G. A. Petersson, H. Nakatsuji, M. Caricato, X. Li, H. P. Hratchian, A. F. Izmaylov, J. Bloino, G. Zheng, J. L. Sonnenberg, M. Hada, M. Ehara, K. Toyota, R. Fukuda, J. Hasegawa, M. Ishida, T. Nakajima, Y. Honda, O. Kitao, H. Nakai, T. Vreven, J. A. Montgomery, Jr., J. E. Peralta, F. Ogliaro, M. Bearpark, J. J. Heyd, E. Brothers, K. N. Kudin, V. N. Staroverov, T. Keith, R. Kobayashi, J. Normand, K. Raghavachari, A. Rendell, J. C. Burant, S. S. Iyengar, J. Tomasi, M. Cossi, N. Rega, J. M. Millam, M. Klene, J. E. Knox, J. B. Cross, V. Bakken, C. Adamo, J. Jaramillo, R. Gomperts, R. E. Stratmann, O. Yazyev, A. J. Austin, R. Cammi, C. Pomelli, J. W. Ochterski, R. L. Martin, K. Morokuma, V. G. Zakrzewski, G. A. Voth, P. Salvador, J. J. Dannenberg, S. Dapprich, A. D. Daniels, O. Farkas, J. B. Foresman, J. V. Ortiz, J. Cioslowski, and D. J. Fox, Gaussian, Inc., Wallingford CT, **2010**.
25 (a) A. S. Esbitt, E. B. Wilson Jr., *Rev. Sci. Instrum.* **1963**, 34, 901-907. (b) G. T. Fraser, R. D. Suenran, C. L. Lugez, *J. Phys. Chem. A* **2000**, 104, 1141-1146.
26 J. C. López, S. Blanco, A. Macario, to be published.
27 L. Evangelisti, S. Tang, B. Velino, W. Caminati, *J. Mol. Structure* **2009**, 912, 285-288.
28 S. Melandri, B. M. Giuliano, A. Maris, L. B. Favero, P. Ottaviani, B. Velino, W. Caminati, *J. Phys. Chem. A* **2007**, 111, 9076-9079.
29 S. Ghosh, J. Thomas, W. Huang, Y. Xu, W. Jäger, *J. Phys. Chem. Letts.* **2015**, 6, 3126-3131.
30 J. K. G. Watson, in *Vibrational Spectra and Structure,* Vol. 6 (Ed: J. R. During), Elsevier, Amsterdam, **1977**, pp. 1-89.
31 O. Desyatnyk, P. Pszczółkowski, S. Thorwirth, T. M. Krygowski, Z. Kisiel, *Phys. Chem. Chem. Phys.* **2005**, 7, 1708-1715.
32 J. Kraitchman, *Am. J. Phys.* **1953**, 21, 17-24.
33 C. C. Costain, *Trans. Am. Crystallogr. Assoc*. 1966, 2, 157–164.
34 J. K. G. Watson, A. Roytburg, W. Ulrich, *J. Mol. Spectrosc.* **1999**, 196, 102-119.
35 G. Gilli, F. Belluci, V. Ferretti, V. Bertolasi, *J. Am. Chem. Soc.* **1989**, 111, 1023-1028.
36 R. Meyer, *J. Mol. Spectrosc.* **1979**, 76, 266−300.
37 R. Meyer, W. Caminati, *J. Mol. Spectrosc.* **1991**, 150, 229−237.
38 R. S. Ruoff, T. D. Klots, T. Emilsson, H. S. Gutowsky, *J. Chem. Phys.* **1990**, 93, 3142-3150.

TABLE OF CONTENTS ENTRY:

The prevalence of the *trans*-COOH form in a hydrated acid complex is shown for the first time in o-anisic acid